

Influence of Nanosegregation on the Surface Tension of Fluorinated Ionic Liquids

Andreia Luís,[†] Karina Shimizu,[‡] João M. M. Araújo,[§] Pedro J. Carvalho,[†] José A. Lopes-da-Silva,^{||} José N. Canongia Lopes,^{*,‡} Luís Paulo N. Rebelo,[§] João A. P. Coutinho,[†] Mara G. Freire,^{*,†} and Ana B. Pereira^{*,§}

[†]Department of Chemistry, CICECO—Aveiro Institute of Materials, University of Aveiro, 3810-193 Aveiro, Portugal

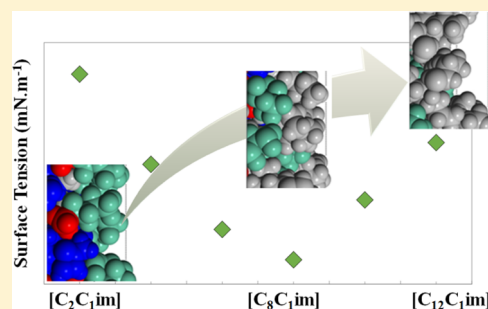
[‡]Centro de Química Estrutural, Instituto Superior Técnico, Universidade de Lisboa, 1049 001 Lisboa, Portugal

[§]Instituto de Tecnologia Química e Biológica António Xavier, Universidade Nova de Lisboa, 2780-157 Oeiras, Portugal

^{||}QOPNA Unit, Department of Chemistry, University of Aveiro, 3810-193 Aveiro, Portugal

Supporting Information

ABSTRACT: We have investigated, both theoretically and experimentally, the balance between the presence of alkyl and perfluoroalkyl side chains on the surface organization and surface tension of fluorinated ionic liquids (FILs). A series of ionic liquids (ILs) composed of 1-alkyl-3-methylimidazolium cations ($[C_nC_1im]$ with $n = 2, 4, 6, 8, 10,$ or 12) combined with the perfluorobutanesulfonate anion was used. The surface tensions of the investigated liquid salts are considerably lower than those reported for non-fluorinated ionic liquids. The most surprising and striking feature is the identification, for the first time, of a minimum at $n = 8$ in the surface tension versus the length of the IL cation alkyl side chain. Supported by molecular dynamics (MD) simulations, it was found that this trend is a result of the competition between the two nonpolar domains (perfluorinated and aliphatic) pointing toward the gas–liquid interface, a phenomenon which occurs in ILs with perfluorinated anions. Furthermore, these ILs present the lowest surface entropy reported to date.



INTRODUCTION

Recently, fluorinated ionic liquids (FILs) have received increasing attention in many fields because of their unique properties. They combine the best properties of ionic liquids (ILs) with those of perfluorocarbons, namely, high gas solubility, low surface tension, relatively low vapor pressure, generally high thermal and chemical stabilities, and easy recovery.^{1–3} The literature related to FILs has mainly focused on their synthesis and their application as reaction media.^{4–8} Other reports have mentioned their outperforming application in electrolytes for fuel and solar cells⁹ and in lithium batteries,¹⁰ as well as in catalysts¹¹ or liquid crystals for optoelectronic applications.¹²

For a thoughtful selection of an adequate IL for a particular application, its thermophysical characterization combined with its property–chemical structure relationship is of key importance. Surface tension is one of the most important properties for the chemical industry and is of vital importance in mass-transfer operations, such as in distillation, extraction, absorption, and adsorption. However, consistent and precise measurements of surface tensions of ILs are difficult because of the presence of surface-active impurities.^{13–21} General trends on surface tensions of ILs according to the chemical structure of the IL,²² alkyl chain length, and cation symmetry²³ have been previously provided and discussed. These papers show that the surface tension of ILs decreases with the increment in the aliphatic alkyl chain length in

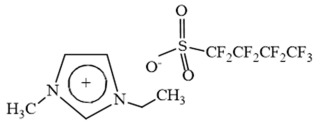
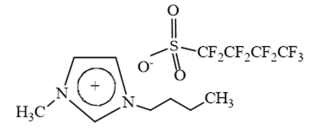
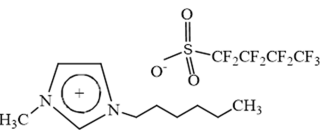
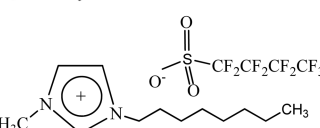
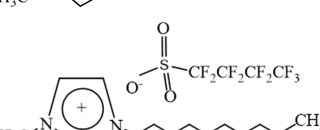
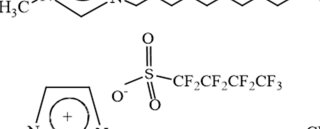
the imidazolium cation until the alkyl chain is not longer than the hexyl chain, where the surface tensions attain an almost constant value.²³

FILs containing fluorinated alkyl chains with at least four carbon atoms can form three nanosegregated domains: one polar and two nonpolar (one aliphatic and the other perfluorinated).²⁴ These domains allow the increase of different conformations, enhancing the diversity of their surfactant behavior.²⁵ Taking into account their particular features, this work aims at expanding the knowledge and understanding of the surface properties of FILs. With this goal in mind, surface tension data of a series of ILs based on the imidazolium cation in the presence of a nonpolar fluorinated moiety attached to the sulfonate group ($[C_nC_1im]-[C_4F_9SO_3]$ with $n = 2, 4, 6, 8, 10,$ or 12) at the anion were determined in the 298–353 K temperature range and at atmospheric pressure. Moreover, the surface thermodynamic functions were determined and the hypothetical critical temperatures were also estimated by means of the Eötvös²⁶ and Guggenheim equations.²⁷ Molecular dynamics (MD) simulations of these FILs were also performed to study the nanoscale structuring and their surface organization, aiming at better

Received: January 21, 2016

Revised: April 8, 2016

Table 1. Chemical Structures and Acronyms of the FILs Used in this Work

FIL Designation	Purification Method	Purity ^c	Water Content ^d	Halides Content	Chemical Structure
1-Ethyl-3-methylimidazolium perfluorobutanesulfonate, [C ₂ C ₁ im][C ₄ F ₉ SO ₃] ^a	Dried under vacuum	0.98 mass fraction ^e	≤ 0.0001 mass fraction	< 0.01 molar fraction ^e	
1-Butyl-3-methylimidazolium perfluorobutanesulfonate, [C ₄ C ₁ im][C ₄ F ₉ SO ₃] ^b	Rotary evaporator and dried under vacuum	0.99 molar fraction	≤ 0.0001 mass fraction	≤ 0.0001 molar fraction ^f	
1-Hexyl-3-methylimidazolium perfluorobutanesulfonate, [C ₆ C ₁ im][C ₄ F ₉ SO ₃] ^a	Dried under vacuum	0.99 mass fraction ^e	≤ 0.0001 mass fraction	< 0.00025 molar fraction ^e	
1-Methyl-3-octylimidazolium perfluorobutanesulfonate, [C ₈ C ₁ im][C ₄ F ₉ SO ₃] ^a	Dried under vacuum	0.99 mass fraction ^e	≤ 0.0001 mass fraction	< 0.00025 molar fraction ^e	
1-Decyl-3-methylimidazolium perfluorobutanesulfonate, [C ₁₀ C ₁ im][C ₄ F ₉ SO ₃] ^b	Rotary evaporator and dried under vacuum	0.99 molar fraction	≤ 0.0001 mass fraction	≤ 0.0001 molar fraction ^f	
1-Dodecyl-3-methylimidazolium perfluorobutanesulfonate, [C ₁₂ C ₁ im][C ₄ F ₉ SO ₃] ^a	Dried under vacuum	0.98 mass fraction ^e	≤ 0.0001 mass fraction	≤ 0.01 molar fraction ^e	

^aSupplied by IoLiTec GmbH. ^bSynthesized in our lab. ^cPurity was determined by NMR. ^dWater content was analyzed by KF titration (Metrohm Ion analysis, 831 KF Coulometer). ^eAs stated by the supplier. ^fNegative for AgNO₃ testing.

understanding the uncommon behavior displayed by these compounds.

EXPERIMENTAL SECTION

Materials. Six FILs were studied in this work: 1-Ethyl-3-methylimidazolium perfluorobutanesulfonate, [C₂C₁im][C₄F₉SO₃], >0.98 mass fraction purity, halides (ion chromatography, IC) <0.01 molar fraction; 1-hexyl-3-methylimidazolium perfluorobutanesulfonate, [C₆C₁im][C₄F₉SO₃], >0.99 mass fraction purity, halides (IC) <0.00025 molar fraction; 1-methyl-3-octylimidazolium perfluorobutanesulfonate, [C₈C₁im][C₄F₉SO₃], >0.99 mass fraction purity, halides (IC) <0.00025 molar fraction; and 1-dodecyl-3-methylimidazolium perfluorobutanesulfonate, [C₁₂C₁im][C₄F₉SO₃], >0.98 mass fraction purity, halides (IC) <0.01 molar fraction. These ILs were supplied by IoLiTec GmbH, and their purity was checked using ¹H and ¹⁹F NMR. 1-Butyl-3-methylimidazolium perfluorobutanesulfonate, [C₄C₁im][C₄F₉SO₃], and 1-decyl-3-methylimidazolium perfluorobutanesulfonate, [C₁₀C₁im][C₄F₉SO₃], were synthesized through the ion exchange resin method. The detailed procedure is described in the [Supporting Information](#). Purity was checked using ¹H and ¹⁹F NMR as well as using elemental analysis. The quantitative integration of their characteristic ¹H and ¹⁹F NMR resonance peaks reveals the expected cation/anion correlations with the use of an internal standard.

Individual samples of each IL were dried at moderate temperature (~323 K) and moderate vacuum (~0.1 Pa) under constant stirring, for a minimum period of 48 h, prior to the measurements to reduce both water and volatile compounds to negligible contents. The water content of each IL, after the drying step and immediately before the measurements, was determined using Karl Fischer (KF) titration making use of a Metrohm 831 Karl Fischer coulometer. The water

content was less than 100 ppm for all of the studied FILs. The IL chemical structures are depicted in [Table 1](#).

Surface Tension. The surface tensions of each IL were determined, in the 298–353 K temperature range, through the analysis of the shape of a pendant drop and measured using a DataPhysics contact angle system OCA-20. Drop volumes of 6 ± 1 μL were obtained using a Hamilton DS 500/GT syringe connected to a Teflon-coated needle placed inside of an aluminum chamber able to maintain the temperature control within ±0.1 K. The temperature was attained by circulating water in a double-jacketed aluminum cell by means of a Julabo F-25 water bath. The temperature inside of the aluminum chamber was measured with a Pt100 probe within ±0.02 K (placed at a distance of approximately 2 cm from the liquid drop). After a specific temperature was reached, the bubble formed and the measurements were carried out after 30 min to guarantee thermal stabilization. Silica gel was placed inside of the closed aluminum chamber 8 h before the surface tension measurements, and the cell was kept sealed during all measurements for a given IL to assure a dry environment. For the determination of surface tension at each temperature and for each IL, at least six drops were formed and measured. For each drop, an average of 200 images were captured. The analysis of the drop shape was executed with the software module SCA 20 in which the gravitational acceleration and latitude were used according to the location of the assay. Density values required for the calculation of the surface tension were taken from previous works.^{3,28} Densities of [C₄C₁im][C₄F₉SO₃] and [C₁₀C₁im][C₄F₁₀SO₃] were determined using an automated SVM3000 Anton Paar rotational Stabinger viscometer–densimeter in the 313.15–353.15 K temperature range and at atmospheric pressure (≈0.1 MPa) and are reported in Table S1 in the [Supporting Information](#). The absolute uncertainty in density is ±(5 × 10⁻⁴) g·cm⁻³, and the relative uncertainty in temperature is within ±0.02 K. The surface tensions of [C₆C₁im]-[C₄F₉SO₃] were determined for temperatures above 303 K, whereas

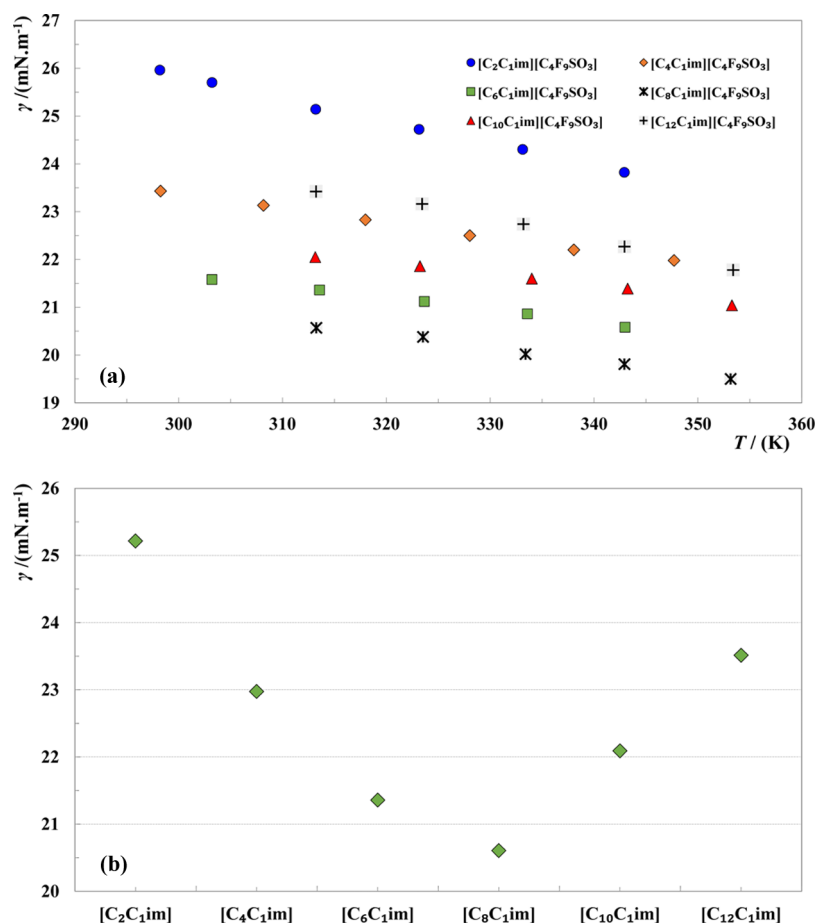


Figure 1. Surface tension as a function of (a) temperature for the studied ILs and (b) the imidazolium alkyl chain size for the $[C_nC_1im][C_4F_9SO_3]$ series ($n = 2, 4, 6, 8, 10,$ and 12) at 313.15 K.

those of $[C_8C_1im][C_4F_9SO_3]$, $[C_{10}C_1im][C_4F_9SO_3]$, and $[C_{12}C_1im][C_4F_9SO_3]$ were determined above 313 K because below these temperatures these ILs are solid. The melting points of $[C_4C_1im][C_4F_9SO_3]$ and $[C_{10}C_1im][C_4F_9SO_3]$ were determined using a DSC Q200 differential scanning calorimeter from TA Instruments following the procedure previously reported^{13,28} and are reported in Table S2 in the Supporting Information; the melting temperatures for the remaining ILs were reported in previous works.^{3,28}

MD Simulations. The interfacial structure of all ILs studied experimentally was probed using MD simulations. The ILs were modeled using the CL&P atomistic force field,²⁹ which is an extension of the assisted model building and energy refinement (AMBER) and optimized potentials for liquid simulation (OPLS) force fields³⁰ specially designed to study ILs and their homologous series. MD simulations were carried out using the DL_POLY 2.20 package.³¹ The runs were performed with a 2 fs time step and a 1.6 nm cutoff distance. Ewald summation corrections were performed beyond the cutoffs. Because of the slow dynamics of this type of system, special care was taken to ensure the attainment of true equilibrium conditions. The number of ion pairs and the size of the simulation box for all studied ILs are presented in Table S3 in the Supporting Information.

All simulations started from low-density configurations that were subjected to 3 ns equilibration runs under isobaric isothermal ensemble conditions at $p = 0.1$ MPa and $T = 343$ K, with Nosé–Hoover thermostats and barostats with relaxation time constants of 1 and 4 ps, respectively. The bulk density of each system reached constant and consistent values, indicating that equilibrium had been attained and that possible ergodicity problems had been overcome. Then, all ILs were re-equilibrated at 298 K for 1.3 ns. Finally, several (at least six) consecutive production stages of 1.0 ns each were performed and the combined

results were used for the evaluation of relevant structural data under bulk conditions.²⁸

To model the IL–vacuum interface, each cubic simulation box containing a pure IL was expanded to a value 3 times its initial size by elongating the sides of the cube along the z -axis. This generated an IL slab with two explicit liquid–vacuum interfaces and tetragonal simulation boxes with approximately $5.0 \times 5.0 \times 20.0$ nm³ dimensions. A simulation run was then conducted under NVT ensemble conditions ($T = 298$ K), with 0.5 and 2 ns equilibration and production stages, respectively; no drift in the studied properties was found from the block analysis of the production stage. To obtain a thicker IL slab, the system was then subjected to a lateral compression (in the x - and y -axes) by running an NpT ensemble simulation for around 150 ps. This process led to a tetragonal box with a 4.0×4.0 nm² base and a liquid layer about 10 nm thick. This configuration was then subjected to new (5.0 ns equilibration + 6 ns production at $T = 353$ K) processes under NVT conditions. The results are discussed below. Possible ergodicity problems were tested by calculating the system properties at different stages of the production runs, including comparisons between slabs of different thicknesses or between processes interspersed by temperature annealing cycles. It should be stressed that, in this work, no surface tension results were calculated by MD simulation. Only the surface structure of the ILs was analyzed using MD simulation results.

RESULTS AND DISCUSSION

Surface Tension. The surface tensions of each FIL are presented in Table S4 in the Supporting Information and depicted in Figure 1. The measured FIL surface tension denotes a temperature dependency commonly observed for ILs.²² The surface tensions of the studied FILs range between 19.49 and

Table 2. Surface Thermodynamic Properties of the FILs

FIL	$10^5(S^\gamma \pm 0.2)$ ($\text{J}\cdot\text{m}^{-2}\cdot\text{K}^{-1}$)	$10^2(H^\gamma \pm 0.08)$ ($\text{J}\cdot\text{m}^{-2}$)
$[\text{C}_2\text{C}_1\text{im}][\text{C}_4\text{F}_9\text{SO}_3]$	4.73	4.00
$[\text{C}_4\text{C}_1\text{im}][\text{C}_4\text{F}_9\text{SO}_3]$	2.99	3.23
$[\text{C}_6\text{C}_1\text{im}][\text{C}_4\text{F}_9\text{SO}_3]$	2.51	2.92
$[\text{C}_8\text{C}_1\text{im}][\text{C}_4\text{F}_9\text{SO}_3]$	2.73	2.92
$[\text{C}_{10}\text{C}_1\text{im}][\text{C}_4\text{F}_9\text{SO}_3]$	2.48	2.99
$[\text{C}_{12}\text{C}_1\text{im}][\text{C}_4\text{F}_9\text{SO}_3]$	4.18	3.66

$26.35 \text{ mN}\cdot\text{m}^{-1}$, presenting values substantially lower than those of other non-fluorinated imidazolium-, pyridinium-, pyrrolidinium-, ammonium-, or phosphonium-based ILs.^{22,32} These low values are similar to those presented by long alkyl chain alkanes, such as dodecane ($25.58 \text{ mN}\cdot\text{m}^{-1}$), tetradecane ($26.69 \text{ mN}\cdot\text{m}^{-1}$), hexadecane ($27.49 \text{ mN}\cdot\text{m}^{-1}$), octadecane ($28.27 \text{ mN}\cdot\text{m}^{-1}$), and eicosane ($28.86 \text{ mN}\cdot\text{m}^{-1}$),³³ or by typical nonionic organic solvents, for example, benzene ($28.88 \text{ mN}\cdot\text{m}^{-1}$), tetrahydrofuran ($26.40 \text{ mN}\cdot\text{m}^{-1}$), dichloromethane ($26.50 \text{ mN}\cdot\text{m}^{-1}$), and cyclohexane ($24.95 \text{ mN}\cdot\text{m}^{-1}$) (surface tension values given at a reference temperature of 293 K)^{34,35} and even aromatic perfluorocarbons, such as perfluorobenzene (C_6F_6 , $21.40 \text{ mN}\cdot\text{m}^{-1}$) and octafluorotoluene (C_7F_8 , $21.12 \text{ mN}\cdot\text{m}^{-1}$) (surface tension values given at a reference temperature of 303 K).¹⁶ On the other hand, these surface tensions are higher than those observed for linear and cyclic nonaromatic perfluorocarbons, such as perfluorohexane (C_6F_{14} , $11.70 \text{ mN}\cdot\text{m}^{-1}$), perfluoroheptane (C_7F_{16} , $13.04 \text{ mN}\cdot\text{m}^{-1}$), perfluorooctane (C_8F_{18} , $14.10 \text{ mN}\cdot\text{m}^{-1}$), perfluorononane (C_9F_{20} , $14.91 \text{ mN}\cdot\text{m}^{-1}$), perfluoro(methylcyclohexane) (C_7F_{14} , $14.54 \text{ mN}\cdot\text{m}^{-1}$), and perfluorodecalin ($\text{C}_{10}\text{F}_{18}$, $18.99 \text{ mN}\cdot\text{m}^{-1}$) (surface tension values given at a reference temperature of 303 K).¹⁶ Similar to that observed for perfluorocarbons,¹⁶ anion fluorination in FILs imposes stronger intramolecular chemical bonds (covalent bonding, the strongest single bond) and weaker van der Waals intermolecular interactions than those of hydrocarbon analogues and thus leading to an important impact on the surface tension of FILs, with FILs displaying in general lower surface tension values than those of most ILs.²²

For a common temperature, for example, 313 K, the surface tension of FILs decreases in the following order: $[\text{C}_2\text{C}_1\text{im}][\text{C}_4\text{F}_9\text{SO}_3] > [\text{C}_{12}\text{C}_1\text{im}][\text{C}_4\text{F}_9\text{SO}_3] > [\text{C}_4\text{C}_1\text{im}][\text{C}_4\text{F}_9\text{SO}_3] > [\text{C}_{10}\text{C}_1\text{im}][\text{C}_4\text{F}_9\text{SO}_3] > [\text{C}_6\text{C}_1\text{im}][\text{C}_4\text{F}_9\text{SO}_3] > [\text{C}_8\text{C}_1\text{im}][\text{C}_4\text{F}_9\text{SO}_3]$. The representation of the surface tension at this temperature as a function of the IL cation alkyl side chain is shown in Figure 1b. Although the increase of the cation aliphatic alkyl chain size, from ethyl up to octyl, leads to a surface tension decrease, as commonly reported for ILs,^{23,36} further increase of the alkyl chain size induces a trend change, with the surface tension increasing with the increase of the alkyl chain size. The same trend is observed for other temperatures as shown in Figure S1 in the Supporting Information. In fact, a minimum occurs at $n = 8$ (for $[\text{C}_8\text{C}_1\text{im}][\text{C}_4\text{F}_9\text{SO}_3]$), shown here for the first time. This behavior is clearly uncommon; for example, the surface tensions of R-alkyl-3-methylimidazolium bis[(trifluoromethyl)sulfonyl]imide ILs ($[\text{C}_n\text{C}_1\text{im}][\text{NTf}_2]$ with $n = 1-16$) decrease with the increase in the cation side aliphatic chain length up to $n = 6$ where it reaches a plateau (an almost constant value up to $[\text{C}_{16}\text{C}_1\text{im}][\text{NTf}_2]$).²³

Surface tension is a measure of the cohesion of liquids, depending therefore on the liquid structure and orientation of the molecules. It is well established that, for many ILs, both the cation and the anion occupy the same plane at the liquid–gas

interface, typically the cation and/or the anion aliphatic moieties projecting toward the interface forming a top layer, whereas the cation polar head groups and those of the anions form the second layer.³⁷ The ILs herein studied are more complex. In particular, FILs based on the perfluorobutanesulfonate anion are known to be able to form three nanosegregated domains, polar, nonpolar aliphatic, and nonpolar fluororous.²⁴ This segregation together with the fluorinated chains presenting lower energy than the aliphatic and the surface tension values on the same range of the perfluorocarbons allows one to envision both the cation and the anion occupying the same plane at the gas–liquid interface but with the perfluorinated chains, instead of the aliphatic, protruding toward the gas phase. This purported surface arrangement changes as the aliphatic imidazolium chain size increases; above an octyl cation alkyl chain size, the aliphatic moieties present lower energy than the perfluorobutyl chain and both the aliphatic and perfluorinated chains protrude toward the gas phase. As the aliphatic chain length further increases, although both structure arrangements may occur at the same time, more aliphatic and less-perfluorinated chains position at the gas–liquid interface, leading to an increase of the surface tension toward non-fluorinated imidazolium IL values. This interpretation is verified and discussed below; see MD Simulations and Langmuir Principle sections.

Surface Thermodynamic Properties. The surface thermodynamic properties, namely, the surface entropy and the surface enthalpy, were derived using the quasi-linear dependence of the surface tension with temperature. The surface entropy, S^γ , and the surface enthalpy, H^γ , can be calculated according to³⁴

$$S^\gamma = -\left(\frac{d\gamma}{dT}\right)_p \quad (1)$$

$$H^\gamma = \gamma - T\left(\frac{d\gamma}{dT}\right)_p \quad (2)$$

where γ stands for the surface tension and T stands for the temperature.

The values of the thermodynamic functions of all ILs investigated are presented in Table 2 and plotted in Figure S2 in the Supporting Information. In general, similarly to what was observed for the surface tensions, the studied FILs present lower surface thermodynamic properties than those of non-FILs.²² These values reveal an extraordinary surface organization as well as a highly structured liquid phase.²⁴ With respect to the values of the surface thermodynamic properties, the FILs investigated display a similar trend as that of the surface tension with a minimum at about $n = 8$ ($[\text{C}_8\text{C}_1\text{im}][\text{C}_4\text{F}_9\text{SO}_3]$; see Figure S2 in the Supporting Information). Furthermore, the surface entropy of these FILs is the lowest obtained for ILs (e.g., ILs based on the imidazolium cation have surface entropies of $0.0673 \text{ mJ}\cdot\text{m}^{-2}\cdot\text{K}^{-1}$ for $[\text{C}_4\text{C}_1\text{im}]\text{Cl}$ ³⁸ or $0.0507 \text{ mJ}\cdot\text{m}^{-2}\cdot\text{K}^{-1}$ for $[\text{C}_6\text{C}_1\text{im}]\text{BF}_4$ ³⁸ and ILs based on quaternary ammonium cations with the bis-(trifluoromethylsulfanyl)imide anion present surface entropies

from 0.0713 to 0.0884 mJ·m⁻²·K⁻¹).³⁹ On the other hand, the solubility capacity of an IL is also governed by its surface tension,^{40,41} and the related surface functions allow us to evaluate this solubility capacity. According to the results obtained, the FILs studied in this work favor high solubility because of their low surface entropy values.^{40,41}

Estimated Critical Temperatures. Critical temperatures (T_c) are one of the most important thermophysical properties because they can be used in many corresponding state correlations regarding the equilibrium and transport properties of fluids.⁴² However, the determination of the IL critical temperatures is a challenging task because ILs decompose at temperatures below the critical point. Although these values are hypothetical quantities, their usefulness is unquestionable, as originally shown for ILs in a previous work.⁴³ IL critical temperatures can typically be estimated using the Eötvös²⁶ or Guggenheim²⁷ relation:

$$\gamma \left(\frac{M}{\rho} \right)^{2/3} = K_{\text{Eot}}(T_{c,\text{Eot}} - T) \quad (3)$$

$$\gamma = K_{\text{Gug}} \left(1 - \frac{T}{T_{c,\text{Gug}}} \right)^{11/9} \quad (4)$$

where γ is the surface tension, $T_{c,\text{Eot}}$ are $T_{c,\text{Gug}}$ are the critical temperature, M is the molecular weight, ρ is the density, and K_{Eot} and K_{Gug} are fitted parameters. Both equations are in accord with the thermodynamic restriction that the surface tension becomes null at the critical point and have proven to provide reasonable estimations.^{42,44} In fact, Rai and Maginn⁴⁵ have shown that the critical temperatures extrapolated by either the Eötvös or Guggenheim method are in good agreement with those obtained by molecular simulation calculations and, therefore, stand as a viable and simple way of estimation. Nonetheless, because the estimation of critical temperatures uses surface tension data from a limited temperature range, it should be highlighted that these critical temperature values (reported in Table 3) must be used with caution. They should be interpreted as semiquantitative.

Table 3. Estimated Critical Temperatures (T_c /K) Using Both the Eötvös (Eot) and the Guggenheim (Gug) Equations^a

FIL	$10^{-3}T_{c,\text{Eot}}$ (K)	$10^{-3}T_{c,\text{Gug}}$ (K)
[C ₂ C ₁ im][C ₄ F ₉ SO ₃]	1.01	0.96
[C ₄ C ₁ im][C ₄ F ₉ SO ₃]	1.51	1.25
[C ₆ C ₁ im][C ₄ F ₉ SO ₃]	1.69	1.35
[C ₈ C ₁ im][C ₄ F ₉ SO ₃]	1.44	1.23
[C ₁₀ C ₁ im][C ₄ F ₉ SO ₃]	1.78	1.40
[C ₁₂ C ₁ im][C ₄ F ₉ SO ₃]	1.06	1.00

^aThe expanded uncertainty with an approximately 95% level of confidence is 100 K.

MD Simulations. MD simulations were used to probe, from a molecular point of view, the IL–vacuum interface of the six members of the [C_{*n*}C₁im][C₄F₉SO₃] homologous series, with $n = 2, 4, 6, 8, 10,$ and $12,$ studied in this work. Each system was modeled considering 8.5–12.9 nm thick slabs of a pure IL limited by two explicit liquid–vacuum boundaries (cf. the Experimental Section for further details). After the equilibration of each slab, the obtained MD trajectories were used to calculate numerical density profile functions of selected IL atoms along the direction (z) normal to the slab surfaces.

Figure 2 depicts such functions in the vicinity of the surface. The liftoff of the numerical density profiles—from their null values in the vacuum subphases to their values in the bulk liquid subphase—were used to set the zero of the z -axis for each surface, with positive z -values always running toward the vacuum subphase. To improve statistics, numerical density values at the same z from the two surfaces were averaged and considered together. The four colored lines correspond to the density profiles of four selected atoms present in the ILs: (i) the CR carbon atom between the two nitrogen atoms of the imidazolium ring, as the representative of the charged moiety of the cation (blue lines), (ii) the SBT atom of the sulfonate group of the anion representing the charged moiety of the anion (red lines), (iii) the CTF terminal carbon atom of the perfluorobutyl chain of the anion representing the nonpolar perfluorobutyl moiety of the anion (green lines), and (iv) the CT terminal carbon atom of the longer alkyl side chain of the cation as a representative of the nonpolar alkyl moiety of the cation (gray lines).

In the case of [C₂C₁im][C₄F₉SO₃] (Figure 2a), the terminal CF₃ groups of the perfluorobutyl chains of the anions (green line) are the ones closer to the outer limits of the surface. One also notices huge oscillations of the numerical density profile functions in the vicinity of the surface, up to at least z -values of ca. -1.2 nm. This applies not only to the perfluorobutyl moieties (green line) but also to the polar moieties of the cation (blue line) and anion (red line). Such oscillations are a consequence of the stratification near the surface of the nanosegregated structure (polar versus nonpolar domains) of the IL;⁴⁶ the outer layer of the surface, which is mainly composed of perfluorobutyl chains, is followed by an inner polar layer composed of interspersed cation- and anion-charged moieties. The methyl groups of the very short ethyl chains of the cation (gray line) necessarily occupy positions in the vicinity of that polar layer, with some groups pointing toward the vacuum and others toward the bulk. Interestingly, the polar layer is followed by yet another inner perfluorobutyl-rich layer (conspicuous green line peak around -1 nm) before the smaller oscillations present in the bulk phase become the norm.

When one considers the other members of the [C_{*n*}C₁im]-[C₄F₉SO₃] homologous series (Figure 2b–f), the most conspicuous feature is the change of the numerical density profiles of the progressively larger alkyl side chains of the cations (gray lines), with peaks closer and closer to the outer layers of the corresponding surfaces. In fact, somewhere between [C₄C₁im]-[C₄F₉SO₃] and [C₆C₁im][C₄F₉SO₃], the profile functions suggest that the outermost nonpolar layers start to be dominated by alkyl chains rather than perfluorobutyl ones. Other features also change, namely, the fact that the oscillations near the surface of all curves become less pronounced for the larger members of the series. It must also be stressed that the apparent decrease in intensity of all peaks is just a consequence of the decreasing numerical density of each of the selected atoms (CR, SBT, CTF, and CT) as the number of other atoms (those present in the alkyl side chains of the cations) are added to the system.

Figure 3 shows snapshots of the simulation boxes with exactly the same length scales of the graphs present in Figure 2. The different atoms were color coded according to a scheme similar to the lines of Figure 2; red represents the charged moiety of the anion (SO₃CF₂–), light green represents the nonpolar moiety of the anion (–CF₂–CF₂–CF₃), blue represents the charged moiety of the cation (CH₃–im–CH₂), and gray represents the nonpolar moiety of the cation (–(CH₂)_{*n*–1}–CH₃).

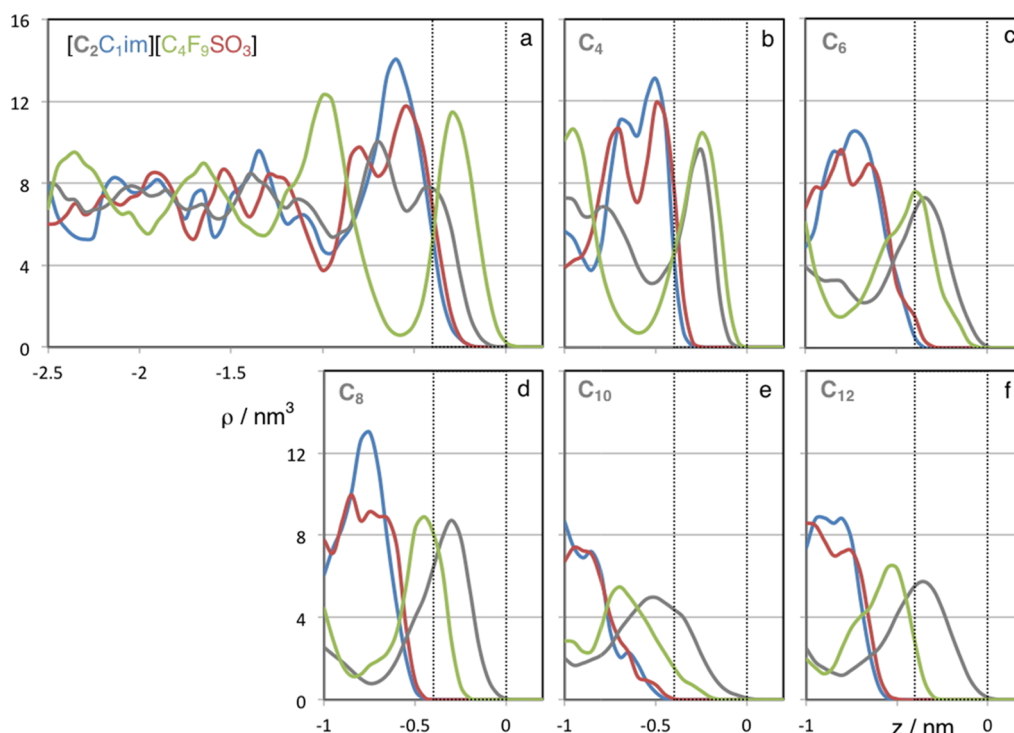


Figure 2. Numerical density profile functions, ρ , along the direction normal to the slab surfaces, z , of four selected atoms of six ILs of the $[\text{C}_n\text{C}_1\text{im}][\text{C}_4\text{F}_9\text{SO}_3]$ series. Green lines: terminal carbon atom of the perfluorobutyl chain of the anions, blue lines: carbon atom between the two nitrogen atoms of the imidazolium ring of the cations, red lines: sulfur atom of the anions, and gray lines: terminal carbon atom of the alkyl side chain of the cations. The region between the dotted lines corresponds to the 0.4 nm thick outer layers of each surface.

Figure 3 shows in a vivid manner the same type of information already present in Figure 2; that is, as the alkyl side chains of the cations get bigger, the surface starts to be replaced by them, in detriment to the perfluorobutyl chains. Another fact is also discernible in the plots; the polar layer gets further away from the outer regions of the surface because of the presence of the longer alkyl chains. For instance, in $[\text{C}_{12}\text{C}_1\text{im}][\text{C}_4\text{F}_9\text{SO}_3]$ (Figure 3f), one cannot see the presence of red and blue atoms from the charged moieties of the ions in the 1 nm thick tier close to the surface.

The unexpected and nonmonotonous trend of the surface tension values obtained in this work can be explained qualitatively by the MD results if one takes into account that the surface tensions of most ILs (especially those without nonpolar side chains) are larger than those of molecular solvents with long aliphatic chains, which in turn exhibit larger surface tension values than those of solvents with fluorinated alkyl chains.²²

For $[\text{C}_2\text{C}_1\text{im}][\text{C}_4\text{F}_9\text{SO}_3]$, the MD density profiles show that the surface is basically composed of the fluorinated and polar layers, and thus the overall surface tension value can be regarded as a result of contributions from the fluorinated chains and from the polar moieties of both ions present in the IL. In the $[\text{C}_4\text{C}_1\text{im}][\text{C}_4\text{F}_9\text{SO}_3]$ system, the butyl chains start to replace the polar layer and push it further away from the outer surface. The surface becomes richer in alkyl moieties at the expense of the polar layer not of the fluorinated one (the latter is the dominant one up to almost $n = 6$ in the $[\text{C}_n\text{C}_1\text{im}][\text{C}_4\text{F}_9\text{SO}_3]$ series). Consequently, there is a drop in the experimental surface tension values because of the replacement at the surface of groups with the largest contributions to the overall surface tension value (the polar moieties of the IL ions) by others with smaller values (the alkyl chains). As the alkyl side chains get longer, they will

continue to push the polar layer away from the surface but eventually will do the same to the fluorinated moieties. At some point, for the larger members of the $[\text{C}_n\text{C}_1\text{im}][\text{C}_4\text{F}_9\text{SO}_3]$ series, the surface tension values will start to increase because of the replacement at the outer surface of the fluorinated groups (with the smallest contributions to the surface tension) by alkyl groups (with larger contributions).

Langmuir Principle. The previous arguments can be explored in a semiquantitative manner if one takes into account the ideas developed by Irwing Langmuir more than 80 years ago.⁴⁷ The Langmuir Principle states that the surface tension is “the result of superposition over the molecule parts present at the outer surface”. The “molecule parts present at the outer surface” can be easily calculated from the numerical density profiles obtained from the MD trajectories or possibly by other surface-sensitive experimental methods such as angle-resolved X-ray photoelectron spectroscopy (ARXPS).⁴⁸ The missing part is the use of an empirical method to estimate the contributions to the surface tension from those molecule parts, which have to be “superpositioned” to obtain the observed surface tension values.

One possibility is to use surface tension to estimate for the different moieties and simply weigh them by their composition (e.g., their volume fractions) at the outer surface. In the present case, the three moieties to be considered are the IL without alkyl side chains (either aliphatic or fluorinated), the aliphatic side chains, and the perfluorinated side chains.

The IL $[\text{C}_1\text{C}_1\text{im}][\text{CF}_3\text{SO}_3]$ can be considered the member of the $[\text{C}_n\text{C}_1\text{im}][\text{C}_m\text{F}_{2m+1}\text{SO}_3]$ homologous series whose side chains are so small that they still belong to the polar moieties of the ions (force-field development studies assisted by ab-initio calculations support this idea²⁹). However, to the best of our knowledge, there are no experimental data for the surface tension of $[\text{C}_1\text{C}_1\text{im}][\text{CF}_3\text{SO}_3]$. For $[\text{C}_2\text{C}_1\text{im}][\text{CF}_3\text{SO}_3]$, the value is

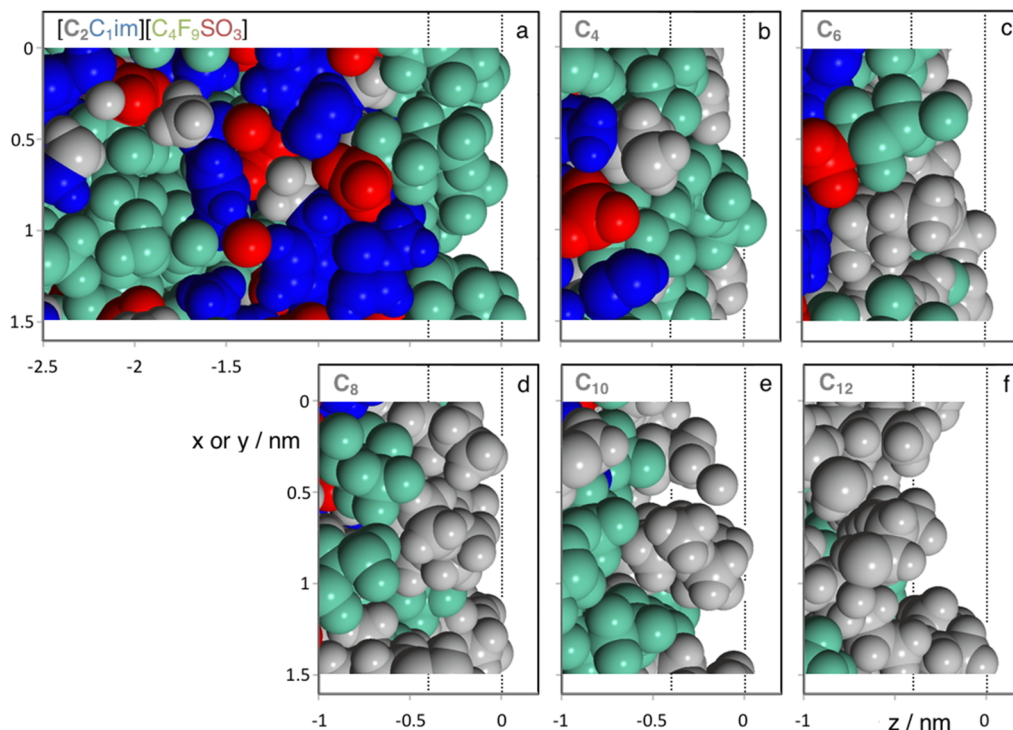


Figure 3. Simulation snapshots of the liquid–vacuum surface of six IL slabs of the $[C_nC_1im][C_4F_9SO_3]$ series. Green atoms: nonpolar moiety ($-CF_2-CF_2-CF_3$) of the perfluorobutyl chains of the anions, blue atoms: imidazolium rings and adjoining atoms of the cations ($CH_3-im-CH_2-$), red atoms: sulfonate groups and adjoining atoms (SO_3CF_2-) of the anions, and gray atoms: nonpolar moiety ($-(CH_2)_{n-2}-CH_3$) of the alkyl side chains of the cations. The length scales and dotted lines are as in Figure 2.

around $39 \text{ mN}\cdot\text{m}^{-1}$ at 353 K.⁴⁹ If one considers the difference in surface tension when the alkyl side chain in the imidazolium is decreased from C_2- to C_1- in other homologous series,²² a reasonable value for the surface tension of $[C_1C_1im][CF_3SO_3]$ would be $40 \text{ mN}\cdot\text{m}^{-1}$ at 353 K. For long aliphatic and fluorinated alkyl chains at the same temperature, the surface tension values tend to cluster around 23 and $12 \text{ mN}\cdot\text{m}^{-1}$, respectively.⁵⁰ It must be stressed that the values estimated for the different moieties are just educated guesses based on available experimental data that try to capture the relative intensity of the contribution of a given moiety to the overall surface tension.

The volume fraction of each moiety at the outer surface layer is calculated in two steps. First, one integrates the numerical density profile functions for each atom representing a moiety between the limit of the surface ($z = 0$) and a stipulated point that marks the thickness of the “outer” surface layer. The representative atoms are CR for the $-C_1C_1im$ moiety, SBT for $-CF_2SO_3$, CT for $C_{n-1}-$, and CTF for C_3F_7- . The dotted lines in Figures 2 and 3 indicate such limits and correspond to a thickness of 0.4 nm. Such a value was set as half of the absolute value of the z -value (0.8 nm) at which the overall numerical density profile within the simulation box starts to deviate from the bulk average numerical density (cf. Figure 4). In other words, the thickness of the outer surface layer is just half of the thickness of the “whole” surface. It must also be stressed that we did not consider any additional schemes such as those that take into account the roughness of the surface, which we deem not necessary given the nature of this semiquantitative approach and its built-in approximations. Second, the atomic numeric fractions thus obtained are converted to moiety volume fractions by taking into account the fact that each of these atoms appears just once in each moiety and that the molar volume of each moiety at 298 K is known from group contribution models.^{28,51}

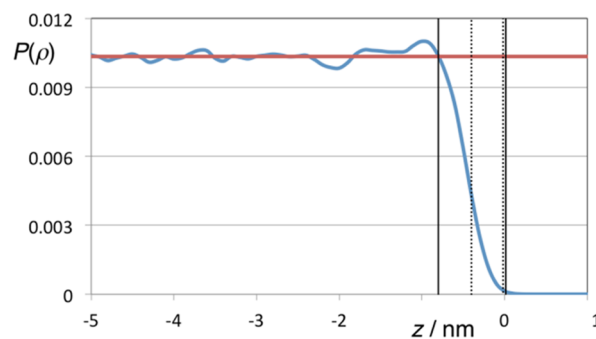


Figure 4. Overall numerical density distribution function, $P(\rho)$, for half of the slab of $[C_2C_1im][C_4F_9SO_3]$. The thickness of the surface (between the full vertical lines) is set as the distance between the takeoff of the density distribution function at $z = 0$ nm and the attainment of densities close to the average bulk values at $z = -0.8$ nm. The thickness of the outer layer of the surface (between the dotted vertical lines) is set as half of that distance, 0.4 nm.

Table 4 shows the results of the integration preconized in the first step (representative atomic numeric fractions at the outer surface) plus the conversion obtained in the second step (moiety volume fractions at the outer surface). It also shows similar results for the bulk (where the representative atomic numeric fractions are 0.25 for each of the four types of atom). The last column of Table 4 combines the composition data with the estimated surface tension contributions of each moiety to estimate the overall surface tension for each system.

The results are compared in Figure 5 with the experimental surface tension data. The agreement between the experimental and “surface” sets can be considered excellent given the number of approximations and degrees of freedom inherent to the

Table 4. Surface Tension Contributions from the Different Moieties Composing the IL Ions^a

[C _n C ₁ im] [C ₄ F ₉ SO ₃] ⁻ , C _n	representative atoms				IL moieties				overall surface tension (mN·m ⁻¹)
	CR	SBT	CE	CTF	-C ₁ C ₁ im	-CF ₂ SO ₃	C _{n-1} -	C ₃ F ₇ -	
					surface tension contribution (mN·m ⁻¹)				
	surface atomic numeric fraction				surface moiety volume fraction				
	40	40	23	12	40	40	23	12	
2	0.14	0.17	0.26	0.43	0.17	0.23	0.07	0.53	24.1
4	0.05	0.10	0.38	0.47	0.06	0.13	0.28	0.54	22.4
6	0.01	0.03	0.55	0.41	0.01	0.04	0.57	0.39	19.5
8	0.00	0.00	0.63	0.37	0.00	0.00	0.72	0.28	20.5
10	0.00	0.00	0.81	0.19	0.00	0.00	0.89	0.11	21.9
12	0.00	0.00	0.88	0.12	0.00	0.00	0.95	0.05	22.4
[C _n C ₁ im] [C ₄ F ₉ SO ₃] ⁻ , C _n	bulk atomic numeric fraction				bulk moiety volume fraction				overall surface tension (mN·m ⁻¹)
2	0.25	0.25	0.25	0.25	0.31	0.33	0.06	0.30	30.7
4	0.25	0.25	0.25	0.25	0.27	0.29	0.17	0.26	29.8
6	0.25	0.25	0.25	0.25	0.25	0.26	0.25	0.23	29.1
8	0.25	0.25	0.25	0.25	0.22	0.24	0.32	0.21	28.5
10	0.25	0.25	0.25	0.25	0.20	0.22	0.38	0.20	28.1
12	0.25	0.25	0.25	0.25	0.19	0.20	0.43	0.18	27.7

^aSurface and bulk compositions of representative atoms and IL moieties. The overall surface tensions are obtained by multiplying the different moiety surface tension contributions by the corresponding (surface or bulk) moiety volume fractions of each IL.

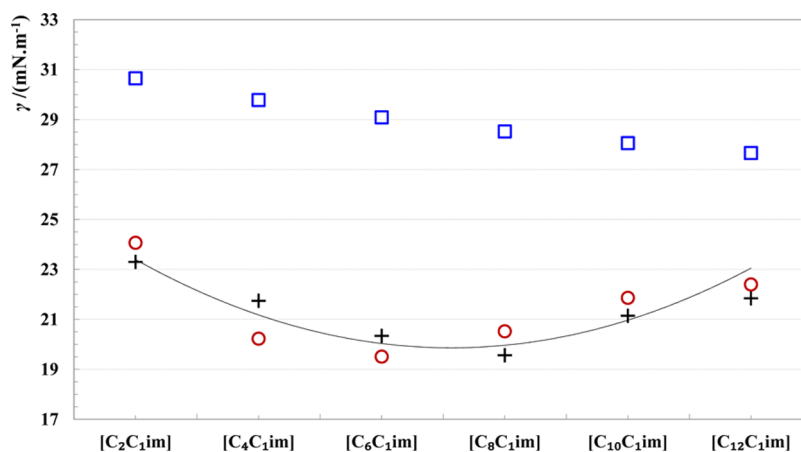


Figure 5. Surface tension values as a function of the alkyl side chain in the [C_nC₁im][C₄F₉SO₃]⁻ IL series. Crosses represent experimental values at 353 K (extrapolated from data in Table S4 in the Supporting Information); red circles represent estimated values taking into account the composition of the outer surface layer of each IL; and blue squares represent estimated values taking into account the bulk composition of each IL.

method. It must be stressed, however, that such agreement can be easily broken if one changes the estimated contributions for the surface tension of the moieties. Nevertheless, the main merit of the present model is to emphasize the fact that the experimental nonmonotonous trend found for the surface tension along [C_nC₁im][C₄F₉SO₃]⁻ cannot be explained by taking into consideration just changes in the bulk composition caused by the increase of the alkyl side chains of the cation—cf. the results from the “bulk” set using the same type of approximation. In other words, the distinct and complex surface concentration patterns along the series, as highlighted by the different numerical density profiles obtained by MD, are the real reason behind the unexpected behavior observed for this particular class of ILs.

CONCLUSIONS

New experimental data of the surface tension of six FILs of the [C_nC₁im][C₄F₉SO₃]⁻ family in the temperature range from 298 to 353 K at atmospheric pressure were determined using the

pendant drop method. The studied FILs present, on average, surface tension values much lower than those reported for non-FILs, presenting the lowest surface tension values reported to date for these types of compounds. FILs also present low surface entropies and surface enthalpies, lower than those of non-FILs. This fact denotes a very high surface organization as well as a markedly structured liquid phase.

The most remarkable finding of this work is a well-defined concave trend in the surface tension versus the alkyl side chain length in the [C_nC₁im][C₄F₉SO₃]⁻ series of ILs, showing a minimum for *n* = 8. This unexpected and nonmonotonous trend of the surface tension values can be rationalized if one takes into account that the surface tensions of most ILs (especially those without nonpolar side chains) are larger than those of molecular solvents with long aliphatic chains, which in turn exhibit larger surface tension values than those of solvents with fluorinated alkyl chains. As one moves from C₂- to C₁₂-, first the surface is basically composed of the fluorinated and polar layers, and then in C₄-, the butyl chains start to replace the polar layer, pushing it

further away from the outer surface. As the alkyl side chains get longer, they will continue to push the polar layer away from the surface and they will do the same to the fluorinated moieties. Thus, for the larger members of the $[C_nC_{1im}][C_4F_9SO_3]$ series, the alkyl groups are the predominant ones at the liquid–gas interface.

The simulation results, which reveal the structure and composition of the liquid–gas interface, together with the estimations based on the Langmuir principle, demonstrate that the competition between aliphatic and fluorinated alkyl chains toward the gas–liquid interface is responsible for the unexpected behavior found in these compounds.

■ ASSOCIATED CONTENT

● Supporting Information

The Supporting Information is available free of charge on the ACS Publications website at DOI: 10.1021/acs.langmuir.6b00209.

Synthesis, characterization, melting points, and densities of $[C_4C_{1im}][C_4F_9SO_3]$ and $[C_{10}C_{1im}][C_4F_9SO_3]$. Surface tension data and surface thermodynamic properties of all fluorinated ionic liquids studied in this work (PDF)

■ AUTHOR INFORMATION

Corresponding Authors

*E-mail: jnlopes@ist.utl.pt (J.N.C.L.).

*E-mail: maragfreire@ua.pt (M.G.F.).

*E-mail: anab@itqb.unl.pt (A.B.P.). Phone: +351 214469471. Fax: +351 214411277.

Notes

The authors declare no competing financial interest.

■ ACKNOWLEDGMENTS

The authors wish to thank FCT/MEC (Portugal) for financial support through grants SFRH/BPD/82264/2011 (P.J.C.) and SFRH/BPD/94291/2013 (K.S.), contracts under Investigator FCT 2014 (A.B.P. and J.M.M.A.), and projects PTDC/QEQ-EPR/5841/2014, PTDC/QEQ-FTT/3289/2014, FCT-ANR/CTM-NAN/0135/2012, IF/00210/2014/CP1244/CT0003, UID/Multi/04551/2013, UID/QUI/00100/2013, and UID/CTM/50011/2013. M.G.F. acknowledges the European Research Council (ERC) for the Starting Grant ERC-2013-StG-337753. The NMR spectrometers are part of The National NMR Facility, supported by FCT/MEC (RECI/BBB-BQB/0230/2012).

■ REFERENCES

- (1) Bara, J. E.; Gabriel, C. J.; Carlisle, T. K.; Camper, D. E.; Finotello, A.; Gin, D. L.; Noble, R. D. Gas separations in fluoroalkyl-functionalized room-temperature ionic liquids using supported liquid membranes. *Chem. Eng. J.* **2009**, *147*, 43–50.
- (2) Zhou, L.; Fan, J.; Shang, X. CO₂ Capture and Separation Properties in the Ionic Liquid 1-*n*-Butyl-3-Methylimidazolium Nonafluorobutylsulfonate. *Materials* **2014**, *7*, 3867–3880.
- (3) Pereiro, A. B.; Araújo, J. M. M.; Martinho, S.; Alves, F.; Nunes, S.; Matias, A.; Duarte, C. M. M.; Rebelo, L. P. N.; Marrucho, I. M. Fluorinated Ionic Liquids: Properties and Applications. *ACS Sustainable Chem. Eng.* **2013**, *1*, 427–439.
- (4) Linder, T.; Sundermeyer, J. Three novel anions based on pentafluorophenyl amine combined with two new synthetic strategies for the synthesis of highly lipophilic ionic liquids. *Chem. Commun.* **2009**, 2914–2916.

- (5) Tindale, J. J.; Mouland, K. L.; Ragogna, P. J. Thiol appended, fluorinated phosphonium ionic liquids as covalent superhydrophobic coatings. *J. Mol. Liq.* **2010**, *152*, 14–18.
- (6) Tsukada, Y.; Iwamoto, K.; Furutani, H.; Matsushita, Y.; Abe, Y.; Matsumoto, K.; Monda, K.; Hayase, S.; Kawatsura, M.; Itoh, T. Preparation of novel hydrophobic fluorine-substituted-alkyl sulfate ionic liquids and application as an efficient reaction medium for lipase-catalyzed reaction. *Tetrahedron Lett.* **2006**, *47*, 1801–1804.
- (7) Xue, H.; Shreeve, J. M. Ionic Liquids with Fluorine-Containing Cations. *Eur. J. Inorg. Chem.* **2005**, 2573–2580.
- (8) Li, X.; Zeng, Z.; Garg, S.; Twamley, B.; Shreeve, J. M. Fluorine-Containing Ionic Liquids from *N*-Alkylpyrrolidine and *N*-Methylpiperidine and Fluorinated Acetylacetones: Low Melting Points and Low Viscosities. *Eur. J. Inorg. Chem.* **2008**, 3353–3358.
- (9) Arvai, R.; Toulgoat, F.; Médebielle, M.; Langlois, B.; Alloin, F.; Jojoui, C.; Sanchez, J. Y. New aryl-containing fluorinated sulfonic acids and their ammonium salts, useful as electrolytes for fuel cells or ionic liquids. *J. Fluor. Chem.* **2008**, *129*, 1029–1035.
- (10) Tsuzuki, S.; Umecky, T.; Matsumoto, H.; Shinoda, W.; Mikami, M. Interactions of Perfluoroalkyltrifluoroborate Anions with Li Ion and Imidazolium Cation: Effects of Perfluoroalkyl Chain on Motion of Ions in Ionic Liquids. *J. Phys. Chem. B* **2010**, *114*, 11390–11396.
- (11) van den Broeke, J.; Winter, F.; Deelman, B.-J.; van Koten, G. A Highly Fluorous Room-Temperature Ionic Liquid Exhibiting Fluorous Biphasic Behavior and Its Use in Catalyst Recycling. *Org. Lett.* **2002**, *4*, 3851–3854.
- (12) Lo Celso, F.; Pibiri, I.; Triolo, A.; Triolo, R.; Pace, A.; Buscemi, S.; Vivona, N. Study on the thermotropic properties of highly fluorinated 1,2,4-oxadiazolopyridinium salts and their perspective applications as ionic liquid crystals. *J. Mater. Chem.* **2007**, *17*, 1201.
- (13) Amat, M. A.; Rutledge, G. C. Liquid–Vapor Equilibria and Interfacial Properties of *n*-Alkanes and Perfluoroalkanes by Molecular Simulation. *J. Chem. Phys.* **2010**, *132*, 114704–114709.
- (14) McLure, I. A.; Soares, V. A. M.; Edmonds, B. Surface Tension of Perfluoropropane, Perfluoro-*n*-butane, Perfluoro-*n*-hexane, Perfluoro-octane, Perfluorotributylamine and *n*-Pentane. *J. Chem. Soc., Faraday Trans. 1* **1982**, *78*, 2251–2257.
- (15) Nishikido, N.; Mahler, W.; Mukerjee, P. Interfacial tensions of perfluorohexane and perfluorodecalin against water. *Langmuir* **1989**, *5*, 227–229.
- (16) Freire, M. G.; Carvalho, P. J.; Queimada, A. J.; Marrucho, I. M.; Coutinho, J. A. P. Surface Tension of Liquid Fluorocompounds. *J. Chem. Eng. Data* **2006**, *51*, 1820–1824.
- (17) Haszeldine, R. N.; Smith, F. Organic fluorides. Part VI. The chemical and physical properties of certain fluorocarbons. *J. Chem. Soc.* **1951**, *16*, 603–608.
- (18) Yoon, J. K.; Burgess, D. J. Comparison of dynamic and static interfacial tension at aqueous/perfluorocarbon interfaces. *J. Colloid Interface Sci.* **1992**, *151*, 402–409.
- (19) Stiles, V. E.; Cady, G. H. Physical Properties of Perfluoro-*n*-hexane and Perfluoro-2-methylpentane. *J. Am. Chem. Soc.* **1952**, *74*, 3771–3773.
- (20) Oliver, G. D.; Blumkin, S.; Cunningham, C. W. Some Physical Properties of Hexadecafluoroheptane. *J. Am. Chem. Soc.* **1951**, *73*, 5722–5725.
- (21) Sakka, T.; Ogata, Y. H. Surface tension of fluoroalkanes in a liquid phase. *J. Fluorine Chem.* **2005**, *126*, 371–375.
- (22) Tariq, M.; Freire, M. G.; Saramago, B.; Coutinho, J. A. P.; Lopes, J. N. C.; Rebelo, L. P. N. Surface tension of ionic liquids and ionic liquid solutions. *Chem. Soc. Rev.* **2012**, *41*, 829–868.
- (23) Almeida, H. F. D.; Freire, M. G.; Fernandes, A. M.; Lopes-da-Silva, J. A.; Morgado, P.; Shimizu, K.; Filipe, E. J. M.; Lopes, J. N. C.; Santos, M. N. B. F.; Coutinho, J. A. P. Cation Alkyl Side Chain Length and Symmetry Effects on the Surface Tension of Ionic Liquids. *Langmuir* **2014**, *30*, 6408–6418.
- (24) Pereiro, A. B.; Pastoriza-Gallego, M. J.; Shimizu, K.; Marrucho, I. M.; Lopes, J. N. C.; Piñeiro, M. M.; Rebelo, L. P. N. On the Formation of a Third, Nanostructured Domain in Ionic Liquids. *J. Phys. Chem. B* **2013**, *117*, 10826–10833.

- (25) Pereira, A. B.; Araújo, J. M. M.; Teixeira, F. S.; Marrucho, I. M.; Piñeiro, M. M.; Rebelo, L. P. N. Aggregation Behavior and Total Miscibility of Fluorinated Ionic Liquids in Water. *Langmuir* **2015**, *31*, 1283–1295.
- (26) Shereshefsky, J. L. Surface Tension of Saturated Vapors and the Equation of Eötvös. *J. Phys. Chem.* **1930**, *35*, 1712–1720.
- (27) Guggenheim, E. A. The Principle of Corresponding States. *J. Chem. Phys.* **1945**, *13*, 253–261.
- (28) Vieira, N. S. M.; Reis, P. M.; Shimizu, K.; Cortes, O. A.; Marrucho, I. M.; Araújo, J. M. M.; Esperança, J. M. S. S.; Lopes, J. N. C.; Pereira, A. B.; Rebelo, L. P. N. A thermophysical and structural characterization of ionic liquids with alkyl and perfluoroalkyl side chains. *RSC Adv.* **2015**, *5*, 65337–65350.
- (29) Canongia Lopes, J. N.; Pádua, A. A. H. CL&P: A generic and systematic force field for ionic liquids modeling. *Theor. Chem. Acc.* **2012**, *131*, 1129–1140.
- (30) Jorgensen, W. L.; Maxwell, D. S.; Tirado-Rives, J. Development and Testing of the OPLS All-Atom Force Field on Conformational Energetics and Properties of Organic Liquids. *J. Am. Chem. Soc.* **1996**, *118*, 11225–11236.
- (31) Smith, W.; Forester, T. R. *The DL_POLY Package of Molecular Simulation Routines* (v.2.2); The Council for The Central Laboratory of Research Councils, Daresbury Laboratory: Warrington, 2006.
- (32) Bhattacharjee, A.; Luís, A.; Santos, J. H.; Lopes-da-Silva, J. A.; Freire, M. G.; Carvalho, P. J.; Coutinho, J. A. P. Thermophysical properties of sulfonium- and ammonium-based ionic liquids. *Fluid Phase Equilib.* **2014**, *381*, 36–45.
- (33) Korosi, G.; Kovats, E. S. Density and surface tension of 83 organic liquids. *J. Chem. Eng. Data* **1981**, *26*, 323–332.
- (34) Adamson, A. W.; Gast, A. P. *Physical Chemistry of Surfaces*, 6th ed; John Wiley, 1997.
- (35) *Surface Tension Values of Some Common Test Liquids for Surface Energy Analysis*, 2006. <http://www.surface-tension.de/> (accessed Dec 16, 2014).
- (36) Santos, C. S.; Baldelli, S. Alkyl chain interaction at the surface of room temperature ionic liquids: systematic variation of alkyl chain length (R = C(1)-C(4), C(8)) in both cation and anion of [RMIM][R-OSO(3)] by sum frequency generation and surface tension. *J. Phys. Chem. B* **2009**, *113*, 923–933.
- (37) Santos, C. S.; Baldelli, S. Gas–liquid interface of room-temperature ionic liquids. *Chem. Soc. Rev.* **2010**, *39*, 2136–2145.
- (38) Ghatee, M. H.; Zolghadr, A. R. Surface tension measurements of imidazolium-based ionic liquids at liquid–vapor equilibrium. *Fluid Phase Equilib.* **2008**, *263*, 168–175.
- (39) Ghatee, M. H.; Bahrami, M.; Khanjari, N. Measurement and study of density, surface tension, and viscosity of quaternary ammonium-based ionic liquids ([N_{222(n)}][Tf₂N]). *J. Chem. Thermodyn.* **2013**, *65*, 42–52.
- (40) Ghatee, M. H.; Bahrami, M.; Khanjari, N.; Firouzabadi, H.; Ahmadi, Y. A Functionalized High-Surface-Energy Ammonium-Based Ionic Liquid: Experimental Measurement of Viscosity, Density, and Surface Tension of (2-Hydroxyethyl)ammonium Formate. *J. Chem. Eng. Data* **2012**, *57*, 2095–2101.
- (41) Bicak, N. A new ionic liquid: 2-hydroxy ethylammonium formate. *J. Mol. Liq.* **2005**, *116*, 15–18.
- (42) Poling, B. E.; Prausnitz, J. M. *The Properties of Gases and Liquids*, 5th ed.; McGraw-Hill, 2000.
- (43) Rebelo, L. P. N.; Lopes, J. N. C.; Esperança, J. M. S. S.; Filipe, E. On the Critical Temperature, Normal Boiling Point, and Vapor Pressure of Ionic Liquids. *J. Phys. Chem. B* **2005**, *109*, 6040–6043.
- (44) Birdi, K. S. *Handbook of Surface and Colloid Chemistry*, 2nd ed.; CRC Press LLC, 2003.
- (45) Rai, N.; Maginn, E. J. Vapor–liquid Coexistence and Critical Behavior of Ionic Liquids via Molecular Simulations. *J. Phys. Chem. Lett.* **2011**, *2*, 1439–1443.
- (46) Nishi, N.; Yasui, Y.; Uruga, T.; Tanida, H.; Yamada, T.; Nakayama, S.-I.; Matsuoka, H.; Kakiuchi, T. Ionic multilayers at the free surface of an ionic liquid, trioctylmethylammonium bis-(nonafluorobutanesulfonyl)amide, probed by X-ray reflectivity measurements. *J. Chem. Phys.* **2010**, *132*, 164705–164716.
- (47) Langmuir, I. Forces Near the Surfaces of Molecules. *Chem. Rev.* **1930**, *6*, 451–479.
- (48) Kolbeck, C.; Lehmann, J.; Lovelock, K. R. J.; Cremer, T.; Paape, N.; Wasserscheid, P.; Fröba, A. P.; Maier, F.; Steinrück, H.-P. Density and Surface Tension of Ionic Liquids. *J. Phys. Chem. B* **2010**, *114*, 17025–17036.
- (49) Součková, M.; Klomfar, J.; Pátek, J. Surface tension of 1-alkyl-3-methylimidazolium based ionic liquids with trifluoromethanesulfonate and tetrafluoroborate anion. *Fluid Phase Equilib.* **2011**, *303*, 184–190.
- (50) Jasper, J. J. The Surface Tension of Pure Liquid Compounds. *J. Phys. Chem. Ref. Data* **1972**, *1*, 841–1009.
- (51) Rebelo, L. P. N.; Lopes, J. N. C.; Esperança, J. M. S. S.; Guedes, H. J. R.; Łachwa, J.; Najdanovic-Visak, V.; Visak, Z. P. Accounting for the Unique, Doubly Dual Nature of Ionic Liquids from a Molecular Thermodynamic and Modeling Standpoint. *Acc. Chem. Res.* **2007**, *40*, 1114–1121.